Dear Editor,

Thank you for your response with regards to our submitted manuscript ("A Silicon Cold Electron Bolometer using Schottky Contacts", reference: L14-04602). We would like to thank both yourself and the reviewer for the time spent in considering the manuscript and for the comments which have been raised.

Firstly, with regards to the comments raised by the editor these have been fully addressed in the updated manuscript and associated files as follows: Figure 2 which had consisted of two separate files for the sub-figures has now been recreated such that the entire figure is contained within a single image file; terms such as 'new' or 'novel' which had been used in the conclusion of the manuscript have been removed and the authors have ensured that the use of acronyms has been reduced to a minimum and that all acronyms have been correctly defined in the first instance. One acronym is still occasionally used, this is 'SINIS' which is used in place of 'superconductor-insulator-normal metal-insulator-superconductor'.

With respect to the reviewer's first point regarding the use of the term 'photon noise limited detection', we emphasise this in the manuscript because we are presenting the first optical measurements with a cold electron bolometer dominated by photon noise. We disagree with the reviewer's comment that achieving photon noise limited performance is necessarily easier in the limit of large optical loading. While a detector can be optimised for an arbitrary background power there are fundamental and practical limits to the sensitivity of the detector at low power levels, which are generally reported as a 'dark' noise equivalent power. At higher levels of optical loading, achieving photon noise limited performance depends upon the detector's properties including the noise sources, the response to absorbed power as well as the optical coupling efficiency, energy and bandwidth of the absorbed photons. For standard bolometers, there is a relationship (described by Richards J. Appl. **76**, 1 (1994)) between temperature of the phonon bath and the ability to optimise a detector for optical noise limited measurement at a given photon frequency independent of the optical power and thus independent of noise equivalent power. For a CEB, the responsivity and sensitivity degrades with increased optical power so that the dark noise equivalent power is not relevant for a device operating with a given optical loading. Due to this relationship between sensitivity with increasing optical power it can in practice be equally difficult to achieve background limited sensitivity under both high and low optical loading.

A demonstration of background limited sensitivity with a detector, at a stated optical power level, frequency and bandwidth, can be more useful figure of merit than a dark noise equivalent power. Specifically in the case of the cold electron bolometer and the data presented in the manuscript the demonstration of background limited performance at the given optical loading and bandwidth is relevant for applications in broadband millimetre-wave imaging systems. This type of optimisation, for cold electron bolometers, has been discussed in the context of balloon-borne cosmic microwave background experiments, such as OLIMPO (Kuzmin *et al.*, J. Phys.: Conf. Ser., **43**, 1298 (2006)).

For the reviewer's second comment regarding the ambiguity of the term 'other detectors', we have adding clarifying text (in parentheses immediately after the use of the phrase 'other cryogenic detectors') to the amended manuscript.

With respect to the third point raised by the reviewer, about the width of the antenna's spectral range: the expected spectral response for a twin-slot type antenna is approximately 50 % of the central frequency of the antenna (as discussed by Focardi, IEEE proc. Antennas and Propagation Society International Symposium, **1**, (2002)). This is in line with our data (shown in Figure 6 of the manuscript).

In response to the reviewer's fourth and fifth points concerning the modelling of the antenna: the initial modelling of the antenna did not allow for the aluminium to be a non-perfect conductor nor did this preliminary model include the lens or the DC cuts in the aluminium ground plane. Since measuring the spectral response of the detector we have repeated our HFSS simulations to account for the non-ideal features of the final antenna structure, that is to say the DC breaks in the aluminium ground plane and treating the aluminium as a non-perfect conductor (typically taking 0.1 Ω/□ or 1 Ω/□). The results of this more recent modelling (shown later in this response) show that when the aluminium is treated as an absorbing material there is a greater level of absorption (in both polarisations) across a broader range frequencies than was seen in the initial model. Our recent modelling also shows that the breaking of the ground plane with the DC cuts (seen in Figure 2b of the manuscript) does result in a slight increase to the response in the polarisation orthogonal that of the twin-slot antenna. It is important to stress that our original intention was not to produce a highly optimised single frequency detector but instead to produce a proof-of-concept detector which was at least partly polarisation sensitive and which had some degree of broadband response. To this end the structure used served its purpose since the optical data obtained show that there is a signal from the cold electron bolometer (clearly present in the vertical polarisation in Figure 6 of the manuscript), our modelling indicates that the broadband response seen in the data can be attributed partially attributed to undesirable losses in the aluminium as well as the effect of the lens, which broadened the range of frequencies absorbed into the cold electron bolometer. One final point on our optical data is that the detector was housed within an aluminium detector block, the inside of this block was not optically black and thus we expect that radiation from our source that was not immediately absorbed by the detector would have been reflected multiple times, altering its polarisation, before being eventually absorbed within the strained silicon. This may further account for some of the *stray* signal seen outside of the expected antenna response and in the orthogonal polarisation.

Our recent modelling has looked at the expected response of the detector, either by using a reverse mode simulation where the power reflected from a lumped port at the antenna feed point (S_{11}) or by measuring the power absorbed when modelling the system in a forward mode. For the forward mode simulations, we have modelled the power absorbed in both the cold electron bolometer and the aluminium (which is assumed to be a non-perfect conductor) in both linear polarisations. The revised simulations have followed a stepped progression from the original idealised case to as realistic a simulation as possible. Specifically we started by re-running our initial model, which assumed the device was illuminated through an infinitely thick silicon layer, this is shown in Figure 1 of this letter. We then replaced this infinite silicon layer with a silicon lens, the results of this simulation are shown in Figure 2. Both of these simulations were performed in a reverse mode where by the detector element was emitting power and the reflected power (S_{11}) was measured. Figure 3 shows the next steps in our simulation which was to take the same model as in the previous case but to perform a

forward mode simulation, whereby the power absorbed from either linear polarisation could be computed in various components. We then introduced the non-ideal features of the detector actually tested; Figure 4 shows the effects of both allowing loss within the aluminium and the breaks in aluminium ground plane.

As already stated, our initial modelling did not include the DC cuts in the aluminium ground plane nor did it allow for loss in the aluminium, furthermore this model assumed that the radiation incident on the antenna was coming through an infinitely thick silicon substrate. The results of this modelling are shown below in Figure 1.

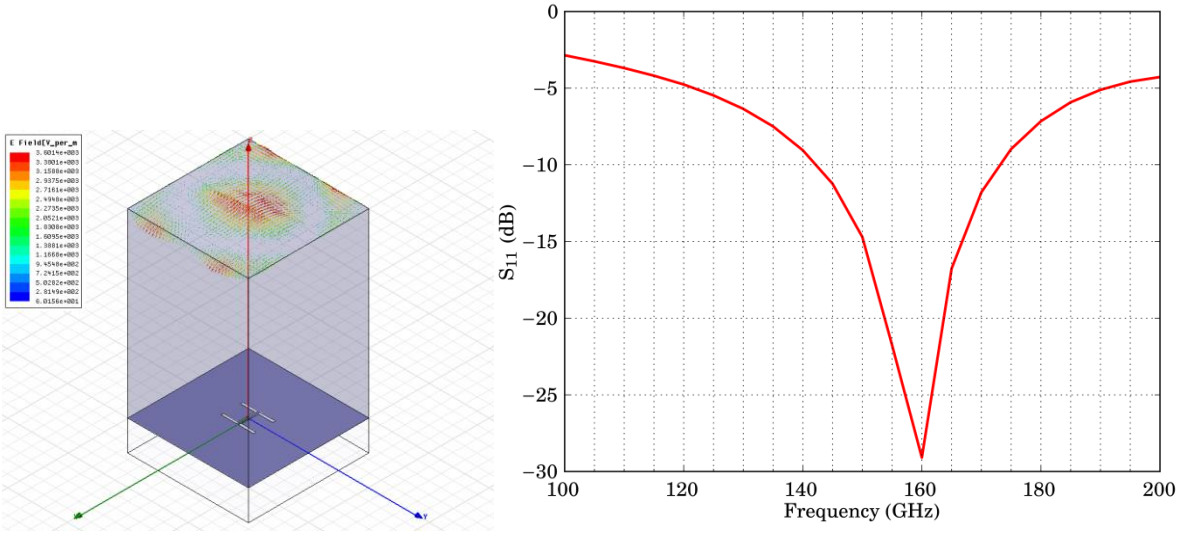

Figure 1: Initial model with infinite silicon substrate Left - HFSS Model. Right – Results of S_{11} modelling in HFSS, the resonance of the antenna is found to be at 160 GHz, as seen in our data (in the manuscript), the 3 dB bandwidth of the antenna is approximately 100 – 200 GHz, thhe 3 dB bandwidth is approximately 10 % of the antenna's resonant frequency.

To update this initial model the first step taken was replace the infinite silicon substrate with a silicon lens (as used in the experiment); this lens was a close approximation to the actual lens used. This situation was simulated both in the reverse direction (studying the S_{11} parameter) and in the forward mode, measuring the power absorbed within the strain silicon cold electron bolometer in both polarisations. This simulation did not explore the effect of either the aluminium being a non-perfect conductor or the breaks in the ground plane.

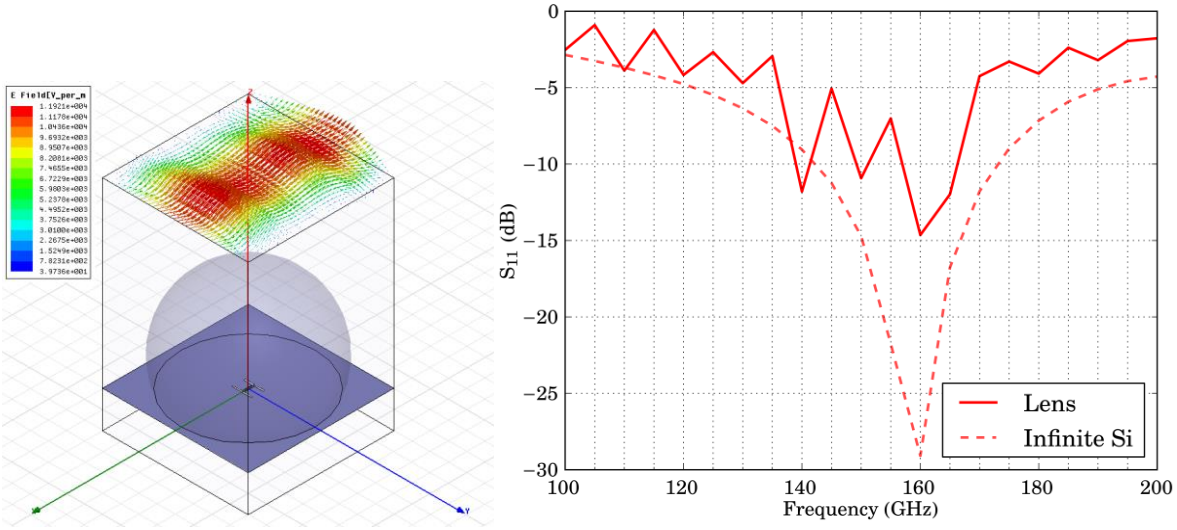

Figure 2: Modelling of antenna with silicon lens hyper-hemispherical lens. Left – HFSS model. Right – S_{11} results for the lens based model (solid line) compared to those seen in Figure 1 (dashed line). It can be seen that there is less power overall reflected and the 3 dB bandwidth is slightly reduced. The degradation of the response is attributed to the fact that the silicon lens is not anti-reflection coated and thus there are multiple reflections from surfaces of the lens

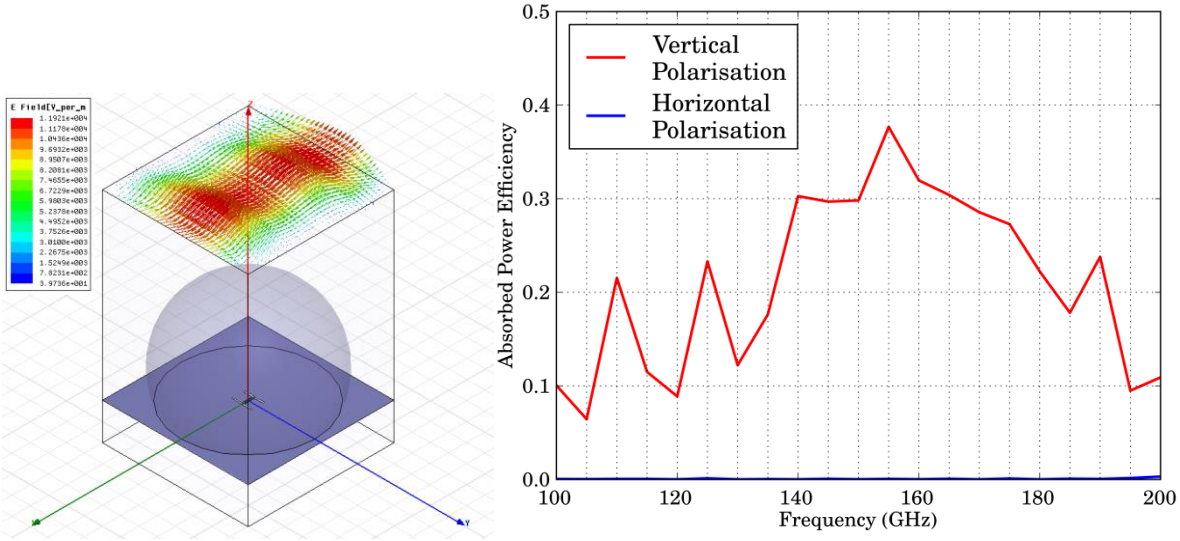

Figure 3: Forward mode modelling of antenna and silicon lens. Left – HFSS model showing electric field strength vectors for the vertical polarisation. Right – Power absorbed (per Watt) within the cold electron bolometer. There is a clear response in the vertical polarisation (red line, defined to be parallel to the antenna), this response is comparable to the S_{11} modelling shown in Figure 3; specifically the 3 dB bandwidth in both simulations seems to be in agreement. There is very little response seen in the horizontal polarisation (blue line).

The final stage of modelling was to incorporate the predicted loss in the aluminium along with the cuts in the ground plane. This simulation also replaced the aluminium extending to the edges of the simulation with a finite area of aluminium and reflection from behind the antenna. Since the forward mode modelling (the type seen in Figure 3) produces more useful information, since the power absorbed in individual components can be measured, this was the only mode of simulation performed in this case.

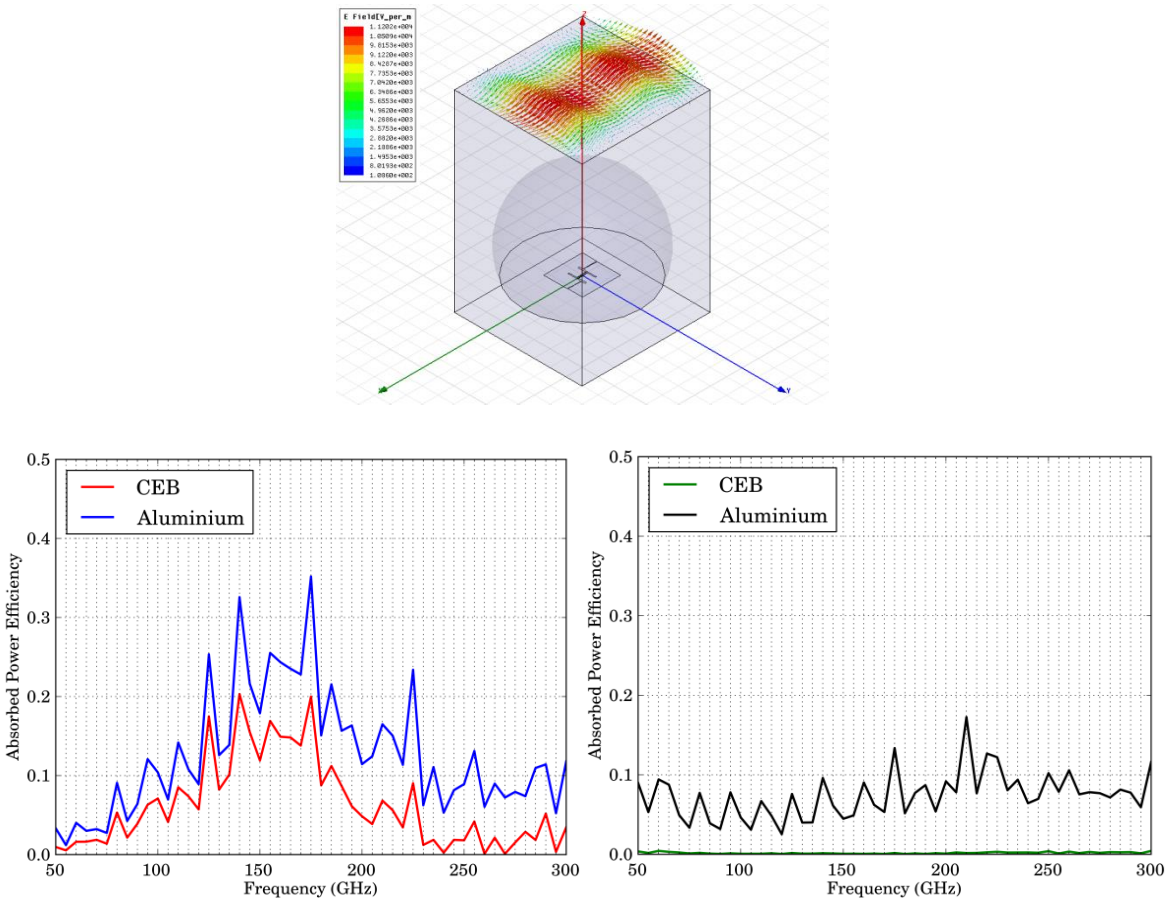

Figure 4: Model of antenna allowing for loss in the aluminium ground plane and the DC breaks in the ground plane. Top – HFSS model with electric field strength, for the vertical polarisation, shown as vectors. Bottom left – Absorption of vertically polarised radiation for the cold electron bolometer (red) and the aluminium (blue, taken to have a resistance of 1 Ω/□). Bottom right – Absorption of horizontally polarised radiation within the cold electron bolometer (green) and the aluminium (black). The additional power absorbed in the aluminium from vertically polarised light is accredited to the currents produced by the antenna in this regime.

It is possible to draw a simple comparison between our data and the modelling by looking at the power absorbed (summed in both polarisations) in both cases. This is shown in Figure 5. From this we see a broad agreement between the data and our modelling, certainly the overall form of the increase in the power being absorbed with increasing frequency, towards the antenna's resonant frequency at 160 GHz, agrees in the two cases, as does the stepped decrease in absorbed power at 225 GHz.

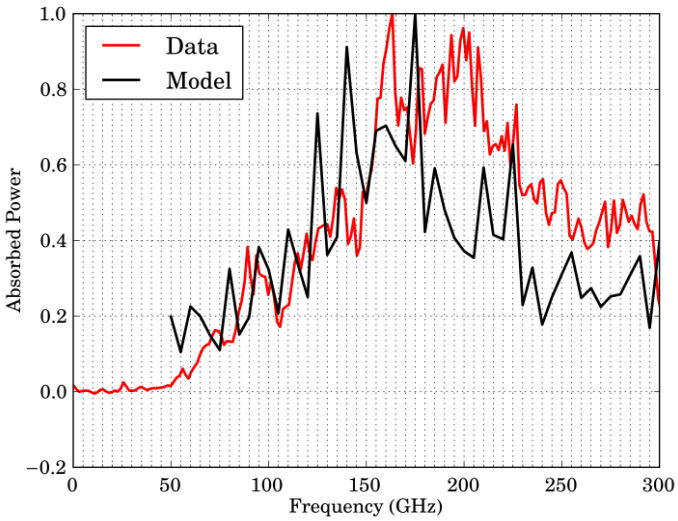

Figure 5: Comparison between total power absorbed in our data (red) and our modelling work (black).

In regards to the sixth point raised by the reviewer, regarding the advantages of a silicon based cold electron bolometers compared to those which utilise a metal absorber: one of the main advantages of a silicon based cold electron bolometer is that, since the tunnelling barrier is formed by the use of Schottky contacts as opposed to an oxide layer (or other insulating layer), the fabrication of this type of device is made simpler. This is analogous to the comparison between metal and silicon based electron coolers described by Savin, Appl. Phys. Lett. **79**, 1471 (2001). The manuscript has been amended (at the start of Section III) to clarify this.

With respect to the seventh point in the reviewer's response, regarding the incomplete set of references given for the optical CEB data, the appropriate references have now been added and are cited within the updated manuscript. We have also added (at the end of the penultimate paragraph of Section V) a brief comparison to noise of the hot electron bolometer type of detector (as reported by Karasik and Cantor, Appl. Phys. Lett. **98**, 193503 (2011)).

On the subject of the comparison between the limiting noise mechanisms for the cold electron bolometer (as reported in our manuscript) and the hot electron bolometer (as reported by Karasik and Cantor (2011)), in both cases, and in the absence of further noise from optical loading, the total noise is a combination of noise from thermal fluctuations in the phonons (within the absorber itself) plus other noise sources associated with the device. These device noise sources are typically dependant on the current or voltage across the device and also strongly dependant on the responsivity. In the case of a hot electron bolometer the sharp superconducting transition, in principle, suppresses these device noise terms at the cost of restricting the range of operational temperature to that of the superconducting transition temperature. In the case of the cold electron bolometer the device noise terms (the 'NIS noise' curve in Figure 1 and terms two through four in Table 1) are approximately equivalent to the phonon noise. However, the cold electron bolometer can operate over a much broader range of both electron and phonon temperatures. In the case of both the cold electron bolometer and the hot electron bolometer the phonon limit to the noise equivalent power is proportional to $\beta\Sigma V T^{\beta+1}$, where Σ is a material constant and V is the volume of the absorber. In the

case of the titanium material used as the absorber in hot electron bolometers the value of the material constant is 1.6×10^9 $\mathrm{WK^{-4}m^{-3}}$ (as stated by Karasik *et al.*, IEEE Trans. on Appl Supercon. **19**, 3 (2009)) whereas the same material constant for a cold electron bolometer using a strain silicon absorber is 2×10^7 $\mathrm{WK^{-6}m^{-3}}$. Furthermore the power of temperature dependency, β, for a cold electron bolometer is 6 (as given by Prest *et al.* (2011)) compared to 4 for the hot electron bolometer (given by Karasik and Cantor (2011)). This, combined with the lower material constant in the strained silicon, means that for the operational temperatures of interest (those below 1 K) the strained silicon cold electron bolometer should offer a much lower phonon noise limit. This can be further seen by comparing, on a per unit volume basis, the thermal conductivity, G, between the electrons and the phonons. The phonon noise limit is proportional to to square root of this quantity. In the case of the cold electron bolometer (at a temperature of 350 mK and using the values given in the submitted manuscript) this is $G_{CEB} = 6.3 \times 10^5$ $\mathrm{WK^{-1}m^{-3}}$, whereas at the same operating temperature the device reported by Karasik and Cantor (2011) has a value of $G_{HEB} = 94 \times 10^7$ $\mathrm{WK^{-1}m^{-3}}$. This shows that the phonon noise limit is expected to be significantly lower in a strained silicon cold electron bolometer.

With regards to the reviewer's eighth point: the main factor which prevented the inclusion of a table of contributions to the overall noise is the space limit of the paper as a whole. We have modelled the expected noise for this device, based upon our I-V and electron temperature measurements (shown in Figure 4 of the manuscript). To estimate the device noise we have followed Golubev and Kuzmin (J. Appl. Phys. **89,** 6464 (2001)). Below is a table showing the estimated contribution to the total noise from various sources at optimum bias.

Table 1: Contributions from various noise sources to the total noise.

Term	**Equation**	**Value**
Amplifier	$\frac{< \delta V^2 >_{amp}}{S^2}$	6.82×10^{-34} $\mathrm{W^2/Hz}$
Electron-Phonon	$2\beta k_B \Sigma \Omega (T_e^{\beta+1} + T_{ph}^{\beta+1})$	2.61×10^{-34} $\mathrm{W^2/Hz}$
Heat Flow	$< \delta P^2 >$	6.23×10^{-34} $\mathrm{W^2/Hz}$
Correlation of Heat Flow and Current	$-2\frac{< \delta P \delta I >}{\frac{\partial I}{\partial V} S}$	8.64×10^{-34} $\mathrm{W^2/Hz}$
Current	$\frac{< \delta I^2 >}{\left(\frac{\partial I}{\partial V} S\right)^2}$	1.35×10^{-33} $\mathrm{W^2/Hz}$
Photon	$2h\nu P_{opt} + \frac{P_{opt}^2}{\delta \nu}$	9.56×10^{-33} $\mathrm{W^2/Hz}$
Total NEP^2	$NEP_{CEB}^2 + NEP_{photon}^2$	1.33×10^{-32} $\mathrm{W^2/Hz}$
Total NEP	$\sqrt{NEP_{CEB}^2 + NEP_{photon}^2}$	1.15×10^{-16} $\mathrm{W/\sqrt{Hz}}$

We have also estimated the expected noise as a function of the voltage across the device, this is shown in Figure 6.

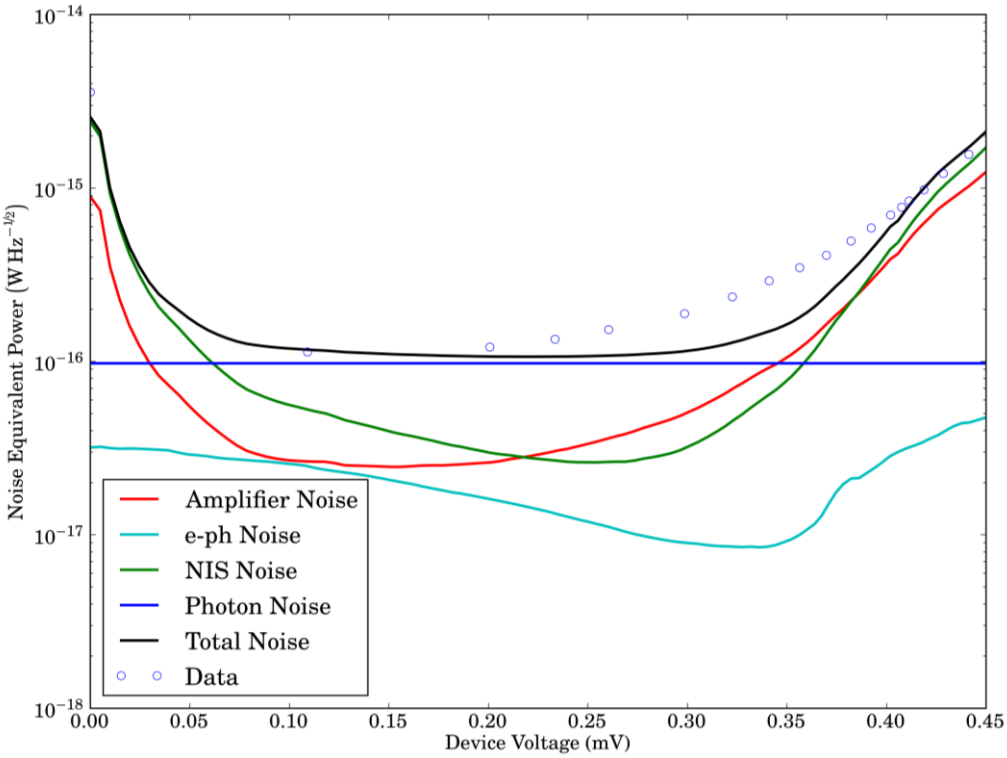

Figure 6: Comparison between measured noise and estimations of contributions from various sources.

The measured noise is consistent with photon noise over a wide range of bias voltages. There is a slight discrepancy between the measured noise (open circles) and the noise model (solid lines) at device voltages around $2\Delta/e$ where the electron temperature is most uncertain. However, the overall form of both the measured noise and the various predictions for the noise contributions is in general agreement with previous predictions for SIN or SIS' devices (for example: Kuzmin, in proc. 17th International Symposium on Space Terahertz Technology (2006) and Kuzmin, J. Low Temp. Phys. **151**, pp. 292-297 (2008)).

Regarding to the reviewer's final point about the ability to use the type of detector described in the manuscript in an imaging array: we have added additional text (in a new second paragraph in Section I) to the manuscript citing Schmidt *et al.*, Appl. Phys. Lett. **86**, 053505 (2005). This paper explains how using a combined radio-frequency and DC biasing signal, along with the frequency domain multiplexing techniques developed for use with kinetic inductance detectors as well as detectors readout using superconductor quantum interference devices, arrays of cold electron bolometers up to hundreds of thousands of pixels can be realised at operating temperatures comparable to that reported in our manuscript.

Once again we would like to thank both yourself and the reviewer for the time spent considering this manuscript and hope that the revisions which we have made, along with the responses in this letter, address the comments raised. We look forward to receiving your comments on the revised manuscript.

For the additional benefit of both the editor and the reviewer we also include an additional PDF file (ReviewerComparision.pdf) which highlights the various changes which have been made.

Yours Faithfully,
Tom Brien